

UC Berkeley

UC Berkeley Previously Published Works

Title

Nanoparticle-Templated Molecular Recognition Platforms for Detection of Biological Analytes

Permalink

<https://escholarship.org/uc/item/2wh242f6>

Journal

Current Protocols in Chemical Biology, 8(3)

ISSN

2160-4762

Authors

Beyene, Abraham G

Demirer, Gozde S

Landry, Markita P

Publication Date

2016-09-01

DOI

10.1002/cpch.10

Peer reviewed

Nanoparticle-Templated Molecular Recognition Platforms for Detection of Biological Analytes

Abraham G. Beyene,^{1,2,3} Gozde S. Demirer,^{1,2,3} and Markita P. Landry^{1,2}

¹Department of Chemical and Biomolecular Engineering, University of California, Berkeley, Berkeley, California

²California Institute for Quantitative Biosciences, QB3, University of California, Berkeley, Berkeley, California

³These authors contributed equally to this work.

Molecular recognition of biological analytes with optical nanosensors provides both spatial and temporal biochemical information. A recently developed sensing platform exploits near-infrared fluorescent single-wall carbon nanotubes combined with electrostatically pinned heteropolymers to yield a synthetic molecular recognition technique that is maximally transparent through biological matter. This molecular recognition technique is known as corona phase molecular recognition (CoPhMoRe). In CoPhMoRe, the specificity of a folded polymer toward an analyte does not arise from a pre-existing polymer-analyte chemical affinity. Rather, specificity is conferred through conformational changes undergone by a polymer that is pinned to the surface of a nanoparticle in the presence of an analyte and the subsequent modifications in fluorescence readout of the nanoparticles. The protocols in this article describe a novel single-molecule microscopy tool (near-infrared fluorescence and total internal reflection fluorescence [nIRF TIRF] hybrid microscope) to visualize the CoPhMoRe recognition process, enabling a better understanding of synthetic molecular recognition. We describe this requisite microscope for simultaneous single-molecule visualization of optical molecular recognition and signal transduction. We elaborate on the general procedures for synthesizing and identifying single-walled carbon nanotube-based sensors that employ CoPhMoRe via two biologically relevant examples of single-molecule recognition for the hormone estradiol and the neurotransmitter dopamine. © 2016 by John Wiley & Sons, Inc.

Keywords: fluorescence microscopy • molecular recognition • near-infrared imaging • nanoparticles • neurotransmitter • nIRF TIRF hybrid microscope • single-walled carbon nanotube (SWCNT) • screening • single molecule imaging • sensors

How to cite this article:

Beyene, A.G., Demirer, G.S., and Landry, M.P. 2016. Nanoparticle-templated molecular recognition platforms for detection of biological analytes *Curr. Protoc. Chem. Biol.* 8:197-223.
doi: 10.1002/cpch.10

INTRODUCTION

Synthetic approaches to molecular recognition have recently grown in prominence as a result of their potential to transform multiple fields of research, including neuroscience, therapeutics, imaging, and drug delivery (Snow et al., 2005; Liu et al., 2009a; Liu et al., 2012; Hong et al., 2015; Oliveira et al., 2015). Optical molecular recognition is critical for



many of these fields due to the importance of simultaneously acquiring spatial and temporal information (for example, concentration profile) about molecular species of interest in their native environment. As a result, the design and successful deployment of synthetic sensing devices can become a key enabler to probing fundamental biological processes within biological systems (Snow et al., 2005; Liu et al., 2012; Zhang et al., 2013).

Molecular recognition—identifying a molecule of interest over other molecular species in complex environments—is but one aspect of a sensing platform. One must also consider signal transduction appropriate for the sensing application of choice. Therefore, any sensing paradigm has to accomplish two things: Recognize a molecule of interest and transduce a signal into a quantifiable readout. In the context of biological applications, this is traditionally accomplished by harnessing the recognition abilities of naturally existing macromolecules such as antibodies (Saerens et al., 2008; Cho et al., 2009). However, the process of purifying significant quantities of antibodies for sensor development is often tedious, expensive, prone to batch variation, and the purified antibodies have limited shelf-life (Peluso et al., 2003; Saerens et al., 2008; Skottrup et al., 2008). Functionalization of nanoparticles with antibodies for sensor development requires processing that could change the chemical structure of the antibody, rendering it ineffective (Peluso et al., 2003; Saerens et al., 2008). Furthermore, ubiquitous use of this method for biomolecule recognition is inherently limited by whether such recognition elements exist. Therefore, the successful development of a rational, high throughput synthetic sensor development paradigm that can circumvent these challenges has implications for vast segments of scientific research. As a result, it has become of paramount interest to visualize the process of molecular recognition on the molecular scale.

Accordingly, nanoparticle-based sensor designs have emerged as attractive platforms to develop molecular recognition devices. While sensing platforms have by and large focused on known molecular recognition elements with electrochemical signal transduction (Adams et al., 2008; Saerens et al., 2008; Cho et al., 2009), in this protocol paper, we focus on the emerging field of corona phase molecular recognition (CoPhMoRe)-based optical nanosensors. CoPhMoRe-based sensors have distinct advantages when (1) natural molecular recognition entities are unavailable and (2) molecular recognition requires both spatial and temporal signal outputs (Zhang et al., 2013; Bisker et al., 2016). To this end, we describe a microscopy platform to study both the polymers that confer molecular recognition and the nanoparticles that provide signal transduction (Landry et al., 2014). In this manner, we can study, with single-molecule resolution (1) the novel synthetic molecular recognition elements based on nanoparticle-templated folded polymers and (2) the optical signal transduction mechanism that is maximally transparent through biological matter.

The central principle of CoPhMoRe is the observation that when heteropolymers are pinned on the surface of a single-walled carbon nanotube (SWCNT), a corona phase forms with unique molecular recognition sites for specific biomolecules (analytes). In the presence of such analytes, the corona phase is perturbed, changing the optical properties of the nanoparticle. It is this modulation in the fluorescent behavior of the nanoparticle that becomes the recognition signal (Fig. 1). It is worth noting that the specificity and sensitivity of sensors that employ CoPhMoRe do not arise out of any known chemical or biological affinity for the analyte, but are instead a result of the conformational changes that the functional polymer undergoes in the presence of an analyte, and the subsequent modifications in fluorescence behavior of the SWCNT. This decoupling of chemical affinity from sensing makes the parameter space for CoPhMoRe sensor development virtually limitless, opening the door for high throughput and rational screening and sensor development. For this reason, it is important to develop optical tools to visualize the process of molecular recognition for successful CoPhMoRe sensors. Incidentally,

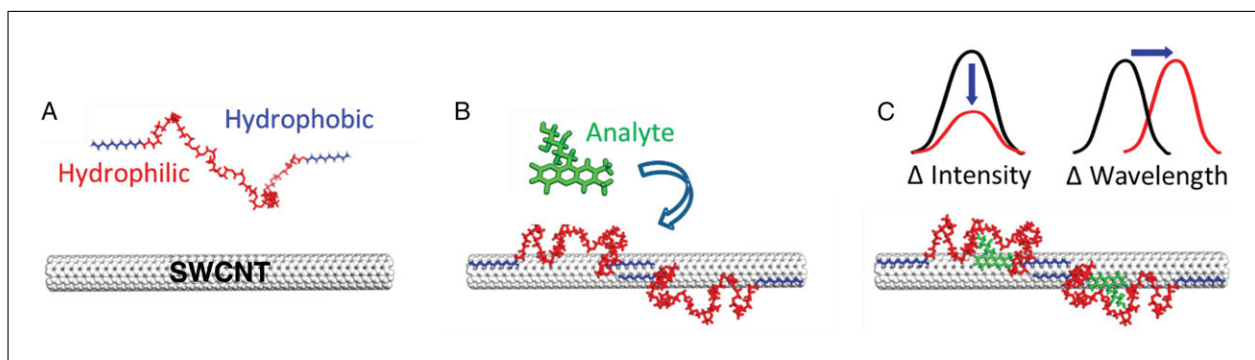


Figure 1 A heteropolymer and SWCNT conjugate pair (A). After the polymer/SWCNT have equilibrated to their minimum free energy configuration (B), the introduction of an analyte results in perturbation of the thermodynamic equilibrium (C), thereby providing a signature emission modulation that can be harnessed for sensing. SWCNT, single-walled carbon nanotube. From Kruss et al., 2014, used with permission from the American Chemical Society.

SWCNTs are near-infrared emissive whereas biological tissue is mostly transparent and has robust photonic lifetimes. These properties lend more credence to the potential that SWCNTs have as sensing platforms.

In this article, Basic Protocol 1 describes the procedure for setting up a single-molecule visible and near-infrared fluorescence microscope (i.e., near-infrared fluorescence and total internal reflection fluorescence [nIRF TIRF] microscopy) to visualize the molecular recognition process itself. We then outline two key examples for identifying CoPhMoRe sensors via screening and subsequent visualization of the molecular recognition process with the nIRF TIRF microscope. Basic Protocol 2 and Support Protocols 1 and 2 describe the corona synthesis and analyte screening for hormone estradiol, whereas Basic Protocol 3 and Support Protocols 3, 4, and 5 detail protocols for the sensing of the neurotransmitter dopamine. Finally, Basic Protocol 4 describes the procedure to test the reversibility of SWCNT-based molecular sensors.

A MICROSCOPIC APPROACH TO STUDY NANOPARTICLE MOLECULAR RECOGNITION CORONAE

The design and characterization of SWCNT-based sensors that take advantage of CoPhMoRe require methods that allow simultaneous optical interrogation of the signal transducer (the SWCNT) and the molecular recognition element (the polymer corona). SWCNTs are best studied using epifluorescence microscopy due to their near-infrared emissivity and the power of the epifluorescence beam through the sample. Conversely, the polymers that surround the nanotube and form a corona are usually not inherently fluorescent and must therefore be tagged with visible fluorophores if one wishes to observe and study their molecular recognition behavior. Such polymer wrappings are best probed using visible wavelength single-molecule microscopy with approaches yielding high signal-to-noise ratios. Total internal reflection fluorescence (TIRF) is especially suited to such molecular level discernment. TIRF enables visualization of surface-adhered molecules of interest within a decaying evanescent field of view roughly 100 nm into the sample. Therefore, a hybrid microscope that encompasses both near-infrared epifluorescence and single-molecule visible fluorescence capabilities is needed to visualize CoPhMoRe-based molecular recognition processes. In this protocol, we describe this hybrid microscope, called nIRF TIRF, with dual channel excitation and emission capabilities. With this hybrid microscope, one can detect the molecular intricacies that occur between the nanoparticle and its corona phase during the process of molecular recognition of a biomolecule. We then demonstrate this microscope's utility in discerning the molecular recognition process for two key analytes: The neurotransmitter dopamine and the hormone estradiol.

BASIC PROTOCOL 1

Nanoparticle Detection of Biological Analytes

199

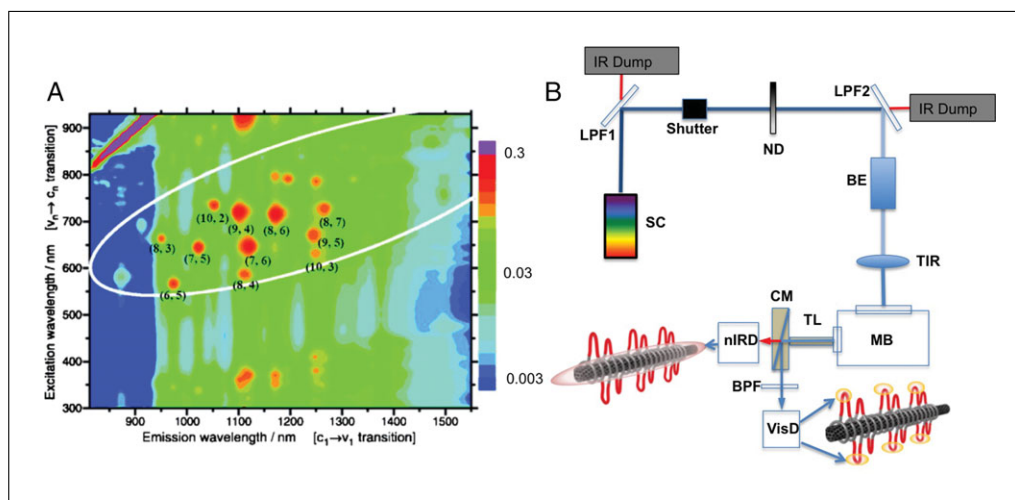


Figure 2 (A) Chirality-dependent photoluminescence of SWCNTs. Reprinted from Bachilo et al., 2002 with permission from the American Association for the Advancement of Science. (B) nIRF TIRF layout and light path: A supercontinuum (SC) laser is attenuated with a neutral density (ND) filter. The beam undergoes $10\times$ beam expansion (BE) to overfill the microscope objective for beam-steering via a plano-convex lens. A collimating lens in the microscope body collects emission while a $2\times$ tube lens expands the image to fill the imaging plane of two detectors. A cold mirror (CM) separates near-infrared and visible light. Visible path: Signal is filtered with a bandpass filter (BPF) and is relayed onto an EM-CCD camera in a single channel 512×512 pixel imaging area. Near-infrared path: Near-infrared emission is directed onto a near-infrared detector at the same imaging plane as the visible detector. SWCNTs, single-walled carbon nanotubes; nIRF TIRF, near-infrared fluorescence and total internal reflection fluorescence; EM-CCD, electron multiplying charge-coupled device; IR, infrared; LPF1, long-pass filter 1; LPF2, long-pass filter 2; TIR, total internal reflection; nIRD, near-infrared detector; TL, tube lens; MB, microscope body; VisD, pixel imaging area. From Bisker et al., 2015, used with permission from the American Chemical Society.

nIRF TIRF Hybrid Microscope

The nIRF TIRF is a hybrid visible/near-infrared microscope that enables simultaneous visualization of SWCNT (via near-infrared fluorescence) and biomolecules (via visible fluorophore-tagged corona phases) with high spatial and temporal resolution. This microscope is used to characterize multi-component SWCNT-biomolecule complexes across a broad range of tunable continuous wavelengths. Broadband excitation is an important feature, because SWCNTs have a broad range of excitation and emission maxima, each peak unique to an individual SWCNT chirality (Bachilo et al., 2002; Fig. 2A). Additionally, fluorophore tags used to visualize CoPhMoRe sensor polymers have a wide range of excitation and emission maxima. Therefore, the nIRF TIRF microscope must capture emission from both SWCNT (nIR) and fluorophores (visible) to simultaneously monitor the sensor signal and the corona phase response to the molecular analyte, respectively (Fig. 2B).

Materials

- Supercontinuum (SC) light source (e.g., NKT EXR-15)
- Shutter (e.g., Thorlabs, cat. no. SH05)
- Two 850-nm long-pass filters (e.g., Semrock, cat. no. FF875-Di01-25 \times 36)
- Neutral density filter set (e.g., Thorlabs, cat. no. FW2AND)
- Plano-convex lens (e.g., Thorlabs, cat. no. LA1256-C)
- Total internal reflection (TIR) lens (e.g., Thorlabs, cat. no. LA1380-C)
- Collimating lens
- Long-pass mirror (e.g., Thorlabs, cat. no. DMLP950)
- Indium gallium arsenide (InGaAs) near-infrared detector
- Bandpass filter (various types, see below)

Electron multiplying charge-coupled device (EM-CCD) camera (e.g., Andor iXon EM-CCD)

CAUTION: While working with the nIRF TIRF microscope, and particularly during its alignment and construction, always wear laser safety goggles and remove any reflective jewelry. The supercontinuum is a Class IV laser, and both direct and scattered beam exposure are hazardous to the eye and skin. To prevent eye exposure, be cognizant of the beam location and be aware of reflected beams. If the beam is not fully enclosed, a nominal hazard zone (NHZ) should be determined and an alarm, warning light, interlock safety system, and verbal countdown should be used during use or start-up of the laser. During initial alignment, tune the laser output to no more than 10% power generation and use temporary neutral density filters along the beam path to minimize beam power. We suggest fully enclosing the laser path, once aligned, to reduce risk of laser-related accidents.

NOTE: Light path and image generation with nIRF TIRF (Fig. 2B): Briefly, the microscope excitation and emission paths are constructed as follows: To excite SWCNTs and visible fluorophores over a broad optical range, the hybrid microscope excitation path uses a supercontinuum (SC) light source. The SC light source is a pseudo-CW fiber laser technology, which emits across a wide range of wavelengths (400 nm to 2400 nm) by coupling a pulsed Ti:sapphire laser with a non-linear photonic crystal fiber (Telford et al., 2009). The high-coherence white light generated is then filtered (Chroma bandpass filters) to selectively produce 480-nm to 800-nm wavelength light for excitation. This range covers the requisite excitation maxima to visualize fluorophores and all excitation peaks of a typical SWCNT multi-chirality sample (Fig. 2A; Bachilo et al., 2002; Miyachi et al., 2004; Salem et al., 2016). A shutter is used to allow illumination only during sampling. The SC light is conditioned through the following series of steps to image near-infrared (nIR) and visible signals (refer to labels in Figure 2B).

1. Mount supercontinuum laser head at the height of the microscope using a laser mount of the user's choice.

The SC laser generates high coherence white light.

Turn the SC laser on at the lowest power setting (~10% output) to create a low-intensity beam. Always use the lowest power setting that will produce a visible beam when aligning the SC laser. At low power output, the beam will appear mostly red in color.

2. Remove any IR region of the white light through the use of two 850-nm long-pass filters (LPF1, LPF2) inserted into the beam path in series.

This is done to prevent saturation of the detector with IR light, which can damage the InGaAs camera. Even stray IR light can overwhelm the near-infrared light emitted from SWCNT sensors. Hence, the leakage of any stray IR light from the excitation path will conflict with photons from the SWCNT and render them undetectable.

3. After the first IR band-pass filtration, pass resulting excitation beam through a neutral density (ND) filter to further attenuate the laser intensity during alignment.

We recommend adjusting this filter wheel to the maximum ND filtration that still enables visualization of the laser beam for alignment.

4. Pass beam through a plano-convex lens (BE) to undergo 10× expansion.

This helps to overfill the microscope objective and expand the field of view.

5. After expansion, use a total internal reflection (TIR) lens to direct the angle of incoming light to the critical angle with respect to the microscope slide such that TIR illumination ~100 nm deep into the sample is achieved.

6. Inside the microscope body (MB), use a filter block turret to hold an excitation filter for the fluorophore and/or SWCNT chirality excitation peak of choice, a band-pass dichroic to separate excitation from emission wavelengths, and a band-pass or long-pass emission filter for the fluorophore or SWCNT chirality of choice.
7. Use a collimating lens at the microscope's exit side port to collect fluorescence emission from the sample and a 2× tube lens (TL) to expand the emitted light to fill the imaging plane of the two detectors: nIR and visible.
8. Use a cold mirror (CM) at the emission port to separate the visible and infrared light emerging from the sample. Reflect fluorescence from fluorophores (400 to 800 nm) to the EM-CCD and nIR SWCNT emissions (900 to 1300 nm) pass through the cold mirror onto an indium gallium arsenide (InGaAs) near-infrared detector (nIRD).
9. Filter visible emissions (450 to 850 nm) from the polymer or its fluorophore through an additional bandpass filter (BPF) to prevent backscattered excitation light from entering the detector. Send resulting beam onto an EM-CCD camera in a 512 × 512 pixel imaging area (VisD).

For more detailed instructions on how to construct a TIRF microscope, see Roy et al., 2008; Joo and Ha, 2012.

BASIC PROTOCOL 2

ANALYTE SCREENING USING CoPhMoRe-BASED OPTICAL NANOSENSORS: TESTING BULK RESPONSE OF RITC-PEG-RITC-SWCNT TO ESTRADIOL

Because CoPhMoRe does not depend on known bio(chemical) affinity for molecular recognition, this platform is fundamentally generic in its ability to produce a sensor for any molecular analyte. However, because the eventual molecular recognition entity (the adsorbed polymer) does not have any pre-existing affinity for the analyte in its desorbed form, a screening approach must be undertaken to identify polymer-nanoparticle conjugates that are selective for a molecular analyte. The process of sensor development therefore involves the following essential steps. First, one must identify a target molecule for which one requires a sensor. In the context of the environment in which this molecule is found, one must develop an analyte library that includes the target molecule, in addition to other likely molecular competitors. A competitor molecule may be a structurally, chemically, functionally, or otherwise similar molecule to the target, or it may be a molecule that is found in large abundance over the target molecule in the environment where molecular detection is to take place. Next, a library of SWCNT-polymer conjugates is synthesized. These SWCNT-polymer conjugates are candidate sensors for the target molecule or analyte. The synthesis of the SWCNT-polymer candidate sensors requires acquiring or synthesizing polymers with hydrophobic anchors that can adsorb onto the nanotube surface and a hydrophilic intermediate that extends into the aqueous phase, forming a colloidally stable suspension of the nanotube (Fig. 3). The SWCNT-polymer conjugates can then be screened against the analyte library. The screening of analytes against the SWCNT-polymer conjugates can yield “hits”—selective optical modulation of the SWCNT fluorescence only upon addition of the target analyte but not upon addition of other competitor molecules in the analyte library. Hits can then be further investigated using the nIRF-TIRF hybrid microscopy technique described in Basic Protocol 1.

Development and Execution of a CoPhMoRe Screen

To demonstrate proof of principle for CoPhMoRe screening, we start with a broad range of small biological molecules as the analyte library. This analyte library is comprised of the 36 biomolecules listed in Table 1. The analyte list is then screened against various SWCNT/polymer conjugate pairs (Table 2) to identify a SWCNT/polymer conjugate selective for one molecule in the analyte library. For an initial screening step such as

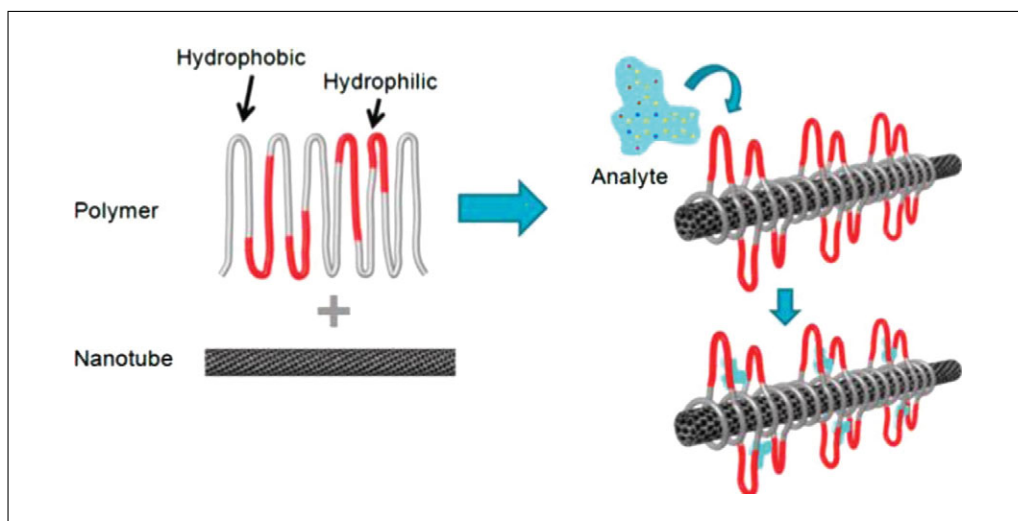


Figure 3 Hydrophobic anchors (gray) adsorbed on SWCNT with hydrophilic segments (red) extending into the aqueous phase. SWCNT, single-walled carbon nanotube; Reproduced from Zhang et al., 2013, with permission from Nature Publishing Group; reproduced from Bisker et al., 2015, with permission from the American Chemical Society.

Table 1 Analyte Library for CoPhMoRe Screening^a

Analyte	Concentration (mM)	Analyte	Concentration (mM)
17- α -Estradiol	0.10	L-Ascorbic Acid	0.50
2,4-Dinitrophenol	0.48	L-Citrulline	0.11
Acetylcholine chloride	0.54	L-Histidine	0.10
α -Tocopherol	0.51	L-Thyroxine	0.10
Adenosine	0.51	Melatonin	0.49
ATP	0.11	NADH	0.51
cAMP	0.10	Quinine	0.01
Creatinine	0.10	Riboflavin	0.10
Cytidine	0.48	Salicylic acid	0.49
D-Aspartic Acid	0.02	Serotonin	0.11
D-Fructose	10.80	Sodium azide	0.51
D-Galactose	5.00	Sodium pyruvate	0.50
D-Glucose	10.90	Sucrose	0.10
D-Mannose	10.30	Thymidine	0.52
Dopamine	0.49	Tryptophan	0.25
Glycine	0.50	Tyramine	0.49
Guanosine	0.51	Urea	0.49
Histamine	0.51		

^aCoPhMoRe, corona phase molecular recognition. Analytes were dissolved in either DMSO or PBS based on solubility. The analyte stock solutions were prepared to achieve final (polymer-nanotube-analyte) concentrations listed in this table. Reproduced from Zhang et al., 2013 with permission from the American Chemical Society.

this, where the desire is to demonstrate CoPhMoRe proof of concept, a wide array of known biomolecules and their analogues can be chosen. If the intent is to develop a sensor for a specific analyte, a more streamlined analyte library comprised of the target molecule and its functional and chemical analogues should be developed (see Basic Protocol 3 below). For the corona phase, heteropolymers are chosen such that they can

Table 2 Polymers Non-Covalently Conjugated to Carbon Nanotubes for the Basis for CoPhMoRe^a

Polymer names	Conjugate names
Rhodamine isothiocyanate (RITC)-difunctionalized polyethylene glycol (PEG)	RITC-PEG-RITC-SWCNT
Fluorescein isothiocyanate (FITC)-difunctionalized polyethylene glycol (PEG)	FITC-PEG-FITC-SWCNT
Distearyl phosphatidylethanolamine (PE) polyethylene glycol	PE-PEG-SWCNT
Fluorenylmethyloxycarbonyl (Fmoc) L-phenylalanine (Phe) polyethylene glycol in a seven-membered brush structure	Fmoc-Phe-PPEG8-SWCNT
Fluorenylmethyloxycarbonyl (Fmoc) L-phenylalanine (Phe) polyethylene glycol in a three membered brush structure	Fmoc-Phe-PPEG4-SWCNT
NH ₂ -PPEG8 in which amine groups replace the Fmoc-Phe groups in the seven membered structure	NH ₂ -PPEG8-SWCNT
Phenoxy (Pho) dextran (Dex)	Pho-Dex-SWCNT
Boronic acid substituted phenoxy dextran	BA-Pho-Dex-SWCNT
Polyvinyl alcohol (PVA)	PVA-SWCNT
(GT) ₁₅ DNA	(GT) ₁₅ -SWCNT
Sodium cholate (SoCh)	SoCh-SWCNT
Sodium dodecyl sulfate (SDS)	SDS-SWCNT

^aAbbreviations: CoPhMoRe, corona phase molecular recognition; SWCNT, single-walled carbon nanotube.

suspend the SWCNTs and form stable colloids. Our previous work suggests a library of polynucleic acids, synthetic peptides, amphiphilic heteropolymers, surfactants, and functionalized phospholipids provides a comprehensive starting point for a molecular recognition screen. Amphiphilic heteropolymers have an adsorbed nonpolar anchor and a desorbed polar chain that extends into the aqueous phase, as depicted in Figure 3.

Analyte library

All analytes used in this screening protocol were purchased from Sigma-Aldrich and prepared as follows: ATP, cAMP, creatinine, D-aspartic acid, glycine, L-citrulline, L-histidine, quinine, sodium pyruvate were dissolved in dimethyl sulfoxide (DMSO). All others were dissolved in 50 mM PBS, pH 7.4. The analytes were dissolved to a final concentration (in polymer-nanotube suspension) shown in Table 1.

Polymer/SWCNT conjugates

All analytes in Table 1 were screened against the nanotube-polymer conjugate pairs provided in Table 2 according to the schematic shown in Figure 4A.

Test bulk response of RITC-PEG-RITC-SWCNT to estradiol

The conjugates listed in Table 2 were placed in a 96-well plate, and the baseline intensity of each SWCNT-polymer conjugate was acquired in triplicate. Subsequently, small concentrated aliquots of each analyte were added to each SWCNT-polymer well. The resulting nIR fluorescence of the nanotube was acquired in triplicate and compared with the pre-analyte response profile. Modulations in fluorescence that were specific and sensitive to a particular analyte were then identified. Modulations can occur in the form of decreased nIR fluorescence, as was the case for RITC-PEG-RITC in response to estradiol (Fig. 4B). Similarly, Fmoc-Phe-PPEG8 showed a selective fluorescence quenching in the presence of L-thyroxine and BA-Pho-Dex recognized riboflavin through an emission wavelength shift. Below, we describe the screening procedure of RITC-PEG-RITC-SWCNT against estradiol. Every other screening pair follows the same procedure.

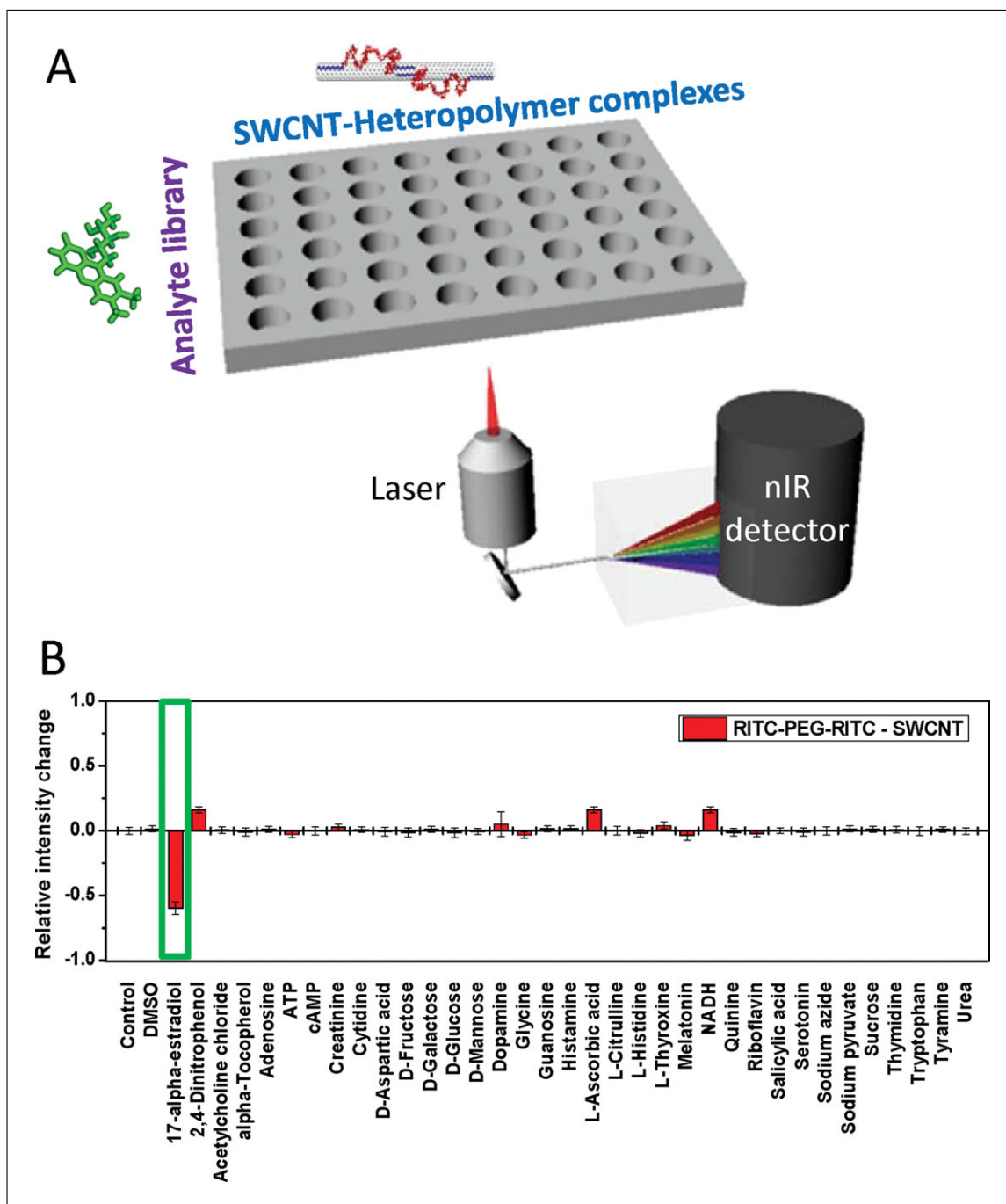


Figure 4 (A) Schematic representation of high throughput screening of analytes for sensor development, in which an analyte library is screened against potential sensors in a well plate. (B) Screening heteropolymer suspended SWCNT against 36 analytes reveals that RITC-PEG-RITC recognizes the hormone estradiol. Note that a good sensing candidate needs to show a distinct optical modulation for a particular analyte, while remaining insensitive to other analytes. SWCNT, single-walled carbon nanotubes; RITC-PEG-RITC, rhodamine isothiocyanate-poly(ethylene) glycol-rhodamine isothiocyanate. Reproduced from Zhang et al., 2013, with permission from Nature Publishing Group.

Materials

50 mM PBS, pH 7.4

RITC-PEG-RITC-SWCNT conjugate (rhodamine isothiocyanate-PEG-rhodamine isothiocyanate-single-walled carbon nanotube conjugate; synthesis provided in Support Protocol 1)

10 mM estradiol solution

96-well plate (Microtest 96 tissue culture plate, BD)
1D OMA V near infrared InGaAs spectrometer (Princeton Instruments)

1. Dilute RITC-PEG-RITC-SWCNT to a final SWCNT concentration of 2 mg/liter in PBS. Compute SWCNT concentration as absorbance at 632 nm divided by 0.036.
2. Aliquot 198 μ l RITC-PEG-RITC-SWCNT solution into an individual well of a 96-well plate.
3. Prepare estradiol stock solution to a final concentration of 10 mM in 50 mM PBS, pH 7.4.

This concentration is chosen such that addition of 2 μ l of the analyte will change the volume of the RITC-PEG-RITC solution by no more than 1%, while yielding a final concentration of 100 μ M estradiol in the 198- μ l aliquot of RITC-PEG-RITC.

4. Measure fluorescence of RITC-PEG-RITC-SWCNT solution before addition of an analyte as described below in step 5. Then add 2 μ l prepared analyte solution and let mixture incubate 1 hr before measuring the final fluorescence.

In this screen, we dissolved analytes (see previous section on analytes) in either DMSO or PBS based on solubility. Most analytes were prepared at a concentration of 500 μ M. Estradiol was prepared at 100 μ M.

5. Measure fluorescence response of RITC-PEG-RITC-SWCNT in triplicate, before and after the addition of estradiol, with an inverted microscope coupled to a spectrometer and an InGaAs OMA V array detector (see Fig. 4A and Supporting Material Fig. 2).

Compute the fluorescence modulation as $(I-I_0)/I_0$ where I_0 is fluorescence before addition of estradiol.

SUPPORT PROTOCOL 1

SYNTHESIS OF RITC-PEG-RITC-SWCNT ESTRADIOL SENSOR

Our screening yielded selective sensors for several small molecule analytes. Among these successful sensors are the RITC-PEG-RITC-SWCNT corona that was shown to have excellent selectivity and sensitivity for the hormone estradiol.

Sensor synthesis requires non-covalent conjugation of polymers onto the surface of carbon nanotubes. Conjugation is commonly carried out by dialysis, bath sonication, or probe-tip sonication. The method of choice depends on the robustness of the polymer and its affinity for the nanotube surface. For example, suspension of polymers robust to probe-tip sonication such as (GT)₁₅ DNA and other short DNA oligonucleotides is performed by sonicating with a 3-mm probe tip for 10 min at 5 W power, followed by centrifugation. Fmoc-Phe-PPEG8 and NH₂-PPEG8 were suspended by sonicating with a 6-mm probe tip for 40 min at 5 W power, followed by centrifugation. Other polymers that may not be able to withstand the harsh conditions of sonication, or that may not have a strong affinity for the nanotube surface are typically suspended by hour-long rounds of bath sonication or dialysis with surfactant-suspended SWCNT as the starting material. We use dialysis to conjugate RITC-PEG-RITC with SWCNT and provide details of polymer synthesis and conjugation below.

Materials

Amine-difunctionalized polyethylene glycol (NH₂-PEG-NH₂, 5 kDa or 20 kDa;
Creative PEGWorks or Nanocs)
Rhodamine isothiocyanate (RITC)
Dichloromethane (CH₂Cl₂)
Dimethylformamide (DMF)
N,N,-Diisopropylethylamine (DIEA)

Diethyl ether (ether)
HiPco single-walled carbon nanotubes (SWCNTs; NanoC or Unidym)
Sodium cholate (SoCh)

Stir bar and stir plate
50-ml Falcon tube
UV-vis-nIR absorption spectrometer (Shimadzu UV-3101PC)
Sonicator (Cole-Parmer)
SW32 Ti rotor (Beckman Coulter)
Centrifuge (Beckman Coulter)
12- to 14-kDa MWCO dialysis bag

Synthesis of RITC-PEG-RITC

1. Mix $\text{NH}_2\text{-PEG-NH}_2$ (0.1 mol/liter) and RITC (0.22 mol/liter) in a 1:1 (v/v) mixture of $\text{CH}_2\text{Cl}_2/\text{DMF}$.
2. Add 0.2 mol/liter DIEA to the reaction mixture.
3. Stir 3 hr with a stir bar on a stir plate at room temperature then precipitate reaction mixture with ether (ten times in volume with respect to the reaction mixture) and re-dissolve in DMF. Repeat cycle two more times.
4. Precipitate reaction mixture in ether and collect purified product through vacuum filtration.
5. Characterize product by UV-vis spectroscopy.

Most polymers can be characterized with UV-vis spectroscopy in the range of 180 to 650 nm. The UV-vis absorption spectrum for characterization of synthesized RITC-PEG-RITC is provided as Supporting Material Figure 5.

Encapsulate carbon nanotubes in RITC-PEG-RITC

6. Add 1 mg/ml NanoC or Unidym nanotubes to 40 ml 2 wt % SoCh in Milli-Q H_2O .

Dry SWCNTs should always be handled in a ventilated hood.

Always wear gloves, lab coat, and eye protection when handling nanotubes and nanotube solutions.

Before using HiPco SWCNTs, extract non-SWCNT material by phase separation in water/hexane mixture as suggested by the manufacturer.

SWCNT purification steps are as follows:

- a. Add 200 to 300 mg unwashed SWCNTs into a 50-ml Falcon tube with 45 ml distilled water.
 - b. Vortex solution 2 min and bath sonicate 5 min.
 - c. Centrifuge solution on floor centrifuge 20 min at maximum speed ($1965 \times g$). Discard water on top and add fresh distilled water.
 - d. Vortex 2 min and then centrifuge again (20 min, $1965 \times g$).
- It is recommended to repeat the vortex and centrifuge steps eight times in order to rinse away all the methanol that is present with the purchased SWCNTs.*
7. Tip-sonicate solution in an ice bath with a 6-mm probe tip at 40% amplitude ($\sim 12\text{ W}$) 1 hr.
 8. Centrifuge resulting dark-black solution in SW32 Ti rotor (Beckman Coulter) at 153,700 RCF (max) 4 hr to remove unsuspended nanotubes.

Check each rotor bucket to ensure it is empty and free of liquid. Even a small particle or droplet in the rotor bucket could lead to off-balance of the rotor during centrifugation and severe damage to the centrifuge and/or rotor unit.

As soon as centrifugation ends, the pellet will begin to dissolve into the decanted solution. Therefore, quick separation of supernatant is required to obtain solution of ONLY single nanotubes, rather than tube bundles.

Aim to keep the top 80% to 90% of the supernatant to avoid disrupting the pellet.

9. Dissolve prepared RITC-PEG-RITC polymer in the SoCh/nanotube suspension to produce a 2 wt % mixture of RITC-PEG(5 kDa)-RITC or 7 wt % mixture of RITC-PEG(20 kDa)-RITC in SoCh-SWCNT suspension.
10. Place mixture in a 12- to 14-kDa MWCO dialysis bag and dialyze against 2 liters 50 mM PBS, pH 7.4, 24 hr to remove free SoCh and to allow the polymer to adsorb on the SWCNT surface. Change dialysis buffer after 12 hr to ensure SoCh removal.

Make sure the appropriate MWCO dialysis membrane is used to retain SWCNT-polymer suspensions.

Optional: In parallel to this, dialysis of SoCh-nanotube suspension (into which no polymer is added) can be set up as a control. Continued removal of SoCh from the suspension will result in the nanotubes precipitating out of the solution, which can be used as a proxy to monitor the extent of dialysis achieved in the SoCh-polymer-nanotube suspension.

11. Record absorption spectrum of the polymer-SWCNT conjugate with a UV-vis-nIR spectrometer and calculate the SWCNT concentration in mg/liter (absorbance at 632 nm/0.036).

A sample UV-vis-nIR absorption spectrum for a multi-chirality DNA-SWCNT sample is provided as Supporting Material Figure 6.

SUPPORT PROTOCOL 2

USING nIRF TIRF TO INTERROGATE CoPhMoRe IN RITC-PEG-RITC-SWCNT

nIRF TIRF hybrid microscopy can be used to elucidate the mechanism of molecular recognition for estradiol. The dual excitation and emission capability of the microscope allows monitoring of the polymer wrapping conformation and the SWCNT nIR signal simultaneously. In this particular case, the RITC anchor is a fluorophore. As such, the polymer does not require exogenous fluorophore tagging for visualization. The RITC domain fluorescence is quenched due to pi-stacking when adsorbed on the SWCNT surface, and regains its fluorescence as it is displaced from the SWCNT surface. Therefore, the visible fluorescence signal from RITC can serve as a “ruler” to measure polymer terminus proximity to the SWCNT surface. Upon introduction of the estradiol, RITC fluorescence increases (Zhang et al., 2013; Kruss et al., 2014). The observed SWCNT emission modulation behavior and the increase in RITC fluorescence occur simultaneously within the frame-rate of our image acquisition (100 msec) upon perfusion of estradiol. This suggests that the analyte displaces a portion of the adsorbed RITC domains and that it is this displacement of the polymer and the subsequent rearrangement of the 3D polymer conformation in the presence of estradiol that enables molecular recognition.

Below, we detail the experimental protocol for surface-immobilizing SWCNT sensors in a microfluidic microscope slide and for visualizing polymer conformation using the nIRF TIRF microscope.

Materials

Pierce BSA-biotin (BSA-Bt; Thermo Fisher Scientific)
NeutrAvidin (Thermo Fisher Scientific)

RITC-PEG-RITC-SWCNT (see Support Protocol 1) or any other conjugate of interest

100 μ M estradiol solution (see Basic Protocol 2) or analyte specific to the polymer-SWCNT conjugate of interest

535-nm narrow-bandpass filter (e.g., Semrock, cat. no. FF01-535/50-25)

562-nm dichroic mirror (e.g., Semrock, cat. no. FF562-Di03-25 \times 36)

585-nm bandpass filter (e.g., Semrock, cat. no. FF01-585/40-25)

Pair of doublet lenses

iXon3 electron multiplying charge coupled device (EMCCD; Andor Technology)

Microfluidic chamber (e.g., Ibidi, sticky-Slide VI 0.4)

1.0 or 1.5 coverslip

Micropipet

Syringe

Microscopy setup to visualize RITC-PEG-RITC conformation on SWCNT upon addition of estradiol

1. Change angle of beam incidence (θ) by moving the TIR lens in the plane perpendicular to beam propagation (Fig. 2B) until the critical angle (θ_c) is reached, at which point all of the incident light is reflected from the surface of glass-water interface and an evanescent field is generated that excites fluorophores in the 100-nm vicinity of the glass-water interface.

The critical angle can be determined using Snell's law:

$$\theta_c = \arcsin \frac{n_r}{n_i}$$

where n_r = the refractive index of the imaging medium (water) and n_i is the refractive index of the incident medium (glass for a glass coverslip, for example).

This excitation method significantly lowers the fluorescence background and allows for high-resolution visualization of dynamic single-molecule behavior.

2. Insert a 535-nm narrow-bandpass filter (FF01-535/50-25, Semrock) before the microscope objective to tune the excitation wavelength relayed to the sample through the objective.

RITC exhibits fluorescence at 572 nm upon excitation by a 547-nm source.

3. Insert a 562-nm dichroic mirror (FF562-Di03-25 \times 36, Semrock) to reflect excitation wavelength while passing the RITC fluorescence emission by allowing the transmission of wavelengths above 562 nm.
4. At the emission port, insert a 585-nm bandpass filter (FF01-585/40-25, Semrock) to reflect the excitation laser light (547 nm) while passing the 572-nm fluorescence emission wavelength of RITC.
5. Use a pair of doublet lenses to expand the 75 \times 75 μ m image to fill the EM-CCD sensor that has dimensions of 8.2 \times 8.2 mm (iXon3 EMCCD, Andor Technology).

Prepare microfluidic chamber and operate nIRF TIRF microscope

6. Prepare microfluidic device: To create microfluidic flow channels, seal sticky side of the Ibidi VI 0.4 slide with a 1.0 or 1.5 coverslip.
7. Introduce micropipet tip to the inlet of a single microfluidic channel and insert syringe into the outlet to flow PBS buffer into the microfluidic channels.

- Flow 50 μ l 10 mg/ml BSA-tagged biotin (BSA-Bt) dissolved in PBS into each microfluidic channel to coat the glass slide surface and the glass coverslip with BSA-Bt.

BSA-Bt serves a dual purpose in passivating the chambers to reduce nonspecific biomolecule adsorption and provides a binding site for NeutrAvidin (Roy et al., 2008).

This is an important step to prevent nonspecific adsorption of the fluorescently tagged biomolecules onto the glass surface.

- Flow PBS buffer through the chambers to rinse non surface-adhered BSA-Bt.
- Flow 0.2 mg/ml NeutrAvidin protein and incubate 10 min to allow binding of NeutrAvidin to the biotin moiety on the surface-bound BSA-Bt.

NeutrAvidin protein binds to the exposed SWCNT surface, which allows for the surface immobilization of the wrapped SWCNT samples.

- Flow in a solution of SWCNT-polymer sensors at a concentration of 1-10 mg/liter in PBS buffer through the channels and incubate 10 min to allow SWCNTs to adsorb to the surface-bound NeutrAvidin.
- Flow in 20 μ l PBS buffer to rinse away non-surface-adsorbed DNA-SWCNTs.
- Place microfluidic slide with surface-immobilized SWCNT sensors on the nIRF TIRF microscope with the coverslip facing the microscope objective. Use a 100 \times objective with oil immersion to visualize individual SWCNT sensors.
- Translate TIR microscope lens until the excitation light is going through the microscope objective and through the sample perpendicular to the microscope slide (epifluorescence mode imaging).
- Find imaging plane of the SWCNT sample by monitoring the nIR emission (i.e., the sensor response) with the InGaAs camera. Acquire an image of the 'before' sensor nIR fluorescence emission.

Make sure the imaging path is set to allow excitation of SWCNT and emission (imaging) of nIR light with appropriate excitation, emission, and dichroic filters.

- Find imaging plane of the fluorophore sample by monitoring the visible emission (i.e., the polymer response) with the EM-CCD camera in TIR mode. Begin by visualizing the sample in epifluorescence mode and adjust excitation beam angle by translating the TIR lens until it reaches a critical angle with respect to the microscope slide. Individual fluorophores will be visualized upon achieving TIR excitation. Acquire image of the 'before' sensor's polymer visible fluorescence emission.

Make sure the imaging path is set to allow excitation of the fluorophore-labeled polymer and emission (imaging) of visible light with appropriate excitation, emission, and dichroic filters specific to that fluorophore.

- Add 20 μ l analyte (e.g., 100 μ M estradiol solution) into the well of the microfluidic slide.

The nIR emission should change as observed during the screening step.

- Repeat step 15 to take an 'after' image of the SWCNT fluorescence and repeat step 16 to take an 'after' image of the polymer fluorescence.
- Overlay 'before' and 'after' analyte channels for the visible and nIR images acquired in steps 15 to 18.

This will allow visualization of fluorophore intensity before and after analyte addition and the corresponding nIRF SWCNT sensor response (Fig. 5).

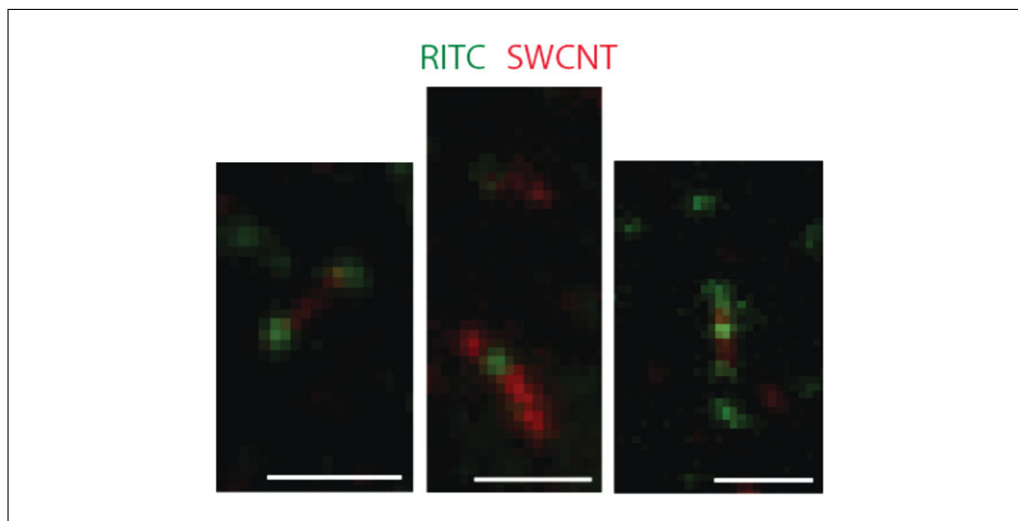


Figure 5 Colocalized RITC molecules (green) and SWCNT (red) are observed after the addition of 500 nM estradiol. Scale 1 μm . RITC, rhodamine isothiocyanate; SWCNT, single-walled carbon nanotubes.

NEUROTRANSMITTER RECOGNITION USING NEUROSENSORS

Neurotransmitters play a central role in complex neural networks by serving as conduits for neuronal communication. As a result, spatiotemporal neurotransmitter sensing has the potential to have a profound impact on our understanding of the brain. However, there are currently few analytical methods to detect neurotransmitter concentration gradients with high spatial and temporal resolution. The brain is composed of complex and delicate tissue and has an abundance of chemical or structural analogues of neurotransmitters, making sensitive detection of the desired neurotransmitters challenging (Perry et al., 2009). Additionally, neurologically relevant processes occur at analytically challenging length (micron) and time (millisecond) scales (Landry et al., 2014).

Electrochemical and fluorescent labeling methods are the most commonly used methods for neurotransmitter detection. While electrochemical methods such as amperometry and voltammetry provide valuable data on dopamine, epinephrine, and serotonin detection, these methods are inherently limited to detect only redox-active neurotransmitters (Adams et al., 2008). Recently, fluorescent labeling methods have provided many opportunities to study neural networks. However, these methods are not capable of directly detecting and visualizing the neurotransmitter itself but rather utilize the structural changes of synaptic cell membranes and vesicles that contain the neurotransmitters (Kim et al., 2011; Rodriguez et al., 2013). Therefore, direct detection of neurotransmitters with high spatial and temporal resolution is still highly needed.

Here, in Basic Protocol 3, we describe a spatially and temporally highly resolved sensor based on SWCNT nIR fluorescence to detect catecholamines with high sensitivity and specificity. SWCNTs have the ability to recognize dopamine when coated with (GT)₁₅ DNA (Kruss et al., 2014). After screening of various SWCNT-polymer conjugates for fluorescence modulation by an analyte library of neurotransmitters, the fluorescence of (GT)₁₅-SWCNTs increases by a factor of 58% to 81% within milliseconds of dopamine exposure in solution (Fig. 6), and over 550% at the single-sensor scale (Fig. 7). Different peaks in nIR fluorescence spectrum correspond to different chiralities of SWCNTs in Figure 6.

Below, we describe a protocol (1) for the development of a candidate SWCNT-polymer nanosensor and analyte screening library and (2) for analyzing fluorescence data obtained from screening.

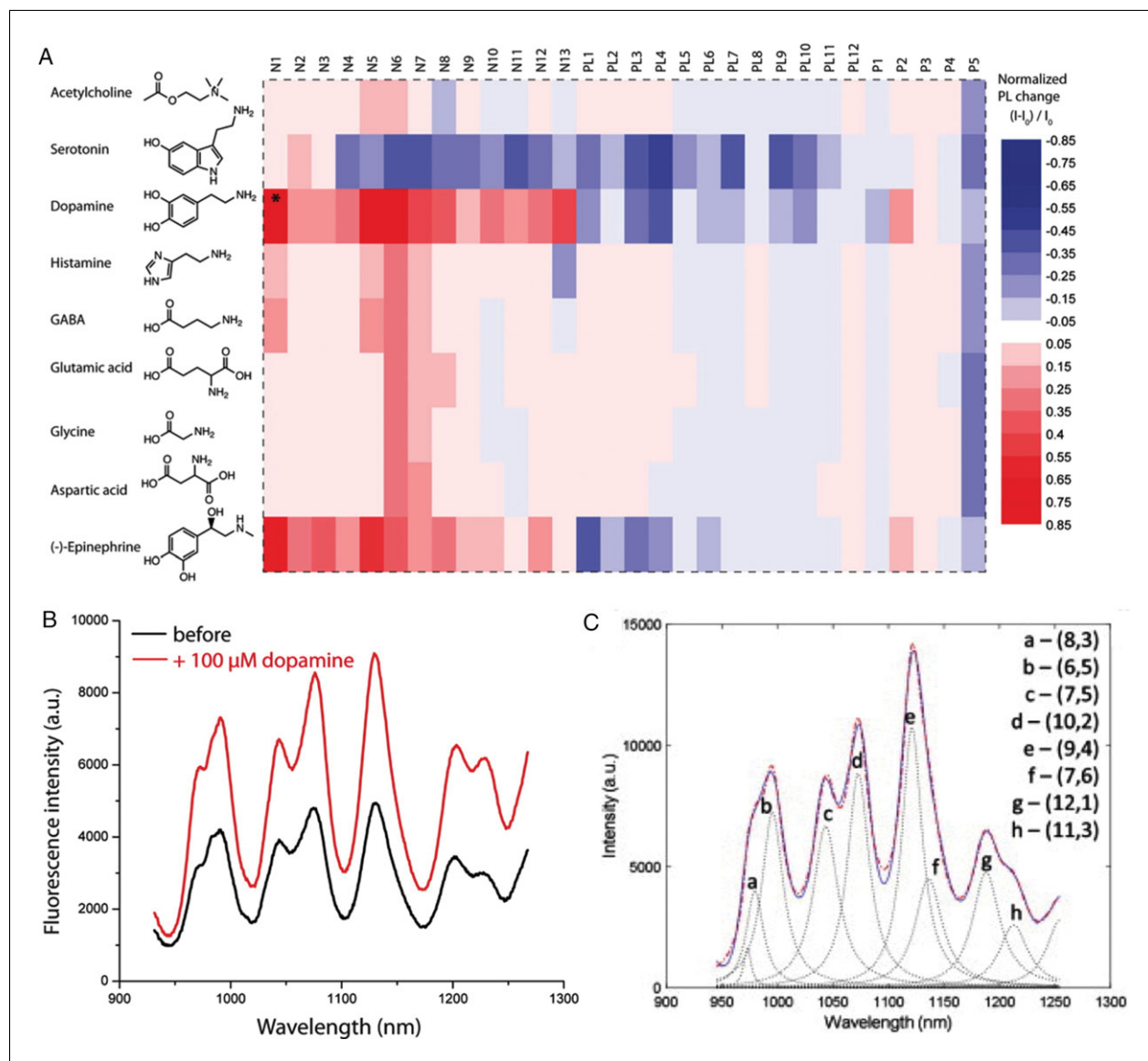


Figure 6 (A) Fluorescence responses of polymer–SWCNT conjugates to analytes (N1 through P5 polymer library can be found in Supporting Material Figure 1; Kruss et al., 2014). (B) nIR fluorescence spectrum (785 nm excitation) of (GT)₁₅–SWCNT before and after addition of 100 μM dopamine in PBS (raw data; Kruss et al., 2014) (C) Deconvolution of a fluorescence spectrum of (GT)₁₅-wrapped SWCNT: Original spectrum (blue curve), individual chirality contributions (dashed black curves) and the sum of the individual peaks (dashed red curve; Salem et al., 2016). SWCNT, single-walled carbon nanotubes; nIR, near infrared.

Development and Execution of a Neurotransmitter (Dopamine) CoPhMoRe Screen

In particular, we focus on dopamine detection in this protocol, as it is one of the central neurotransmitters in the brain. Our neurotransmitter screening library consists of 9 analytes and 30 different candidate nanosensors. The analyte library contains molecules with structural or functional homology to dopamine that can interfere with dopamine detection. Dopamine is typically detected electrochemically, based on redox chemistry (Kruss et al., 2014). Therefore, we include molecules with similar redox potentials to dopamine in our analyte library, along with molecules found in abundance in brain tissue: Acetylcholine, serotonin, histamine, γ -aminobutyric acid (GABA), glutamic acid, glycine, aspartic acid, and (-)-epinephrine (Fig. 6A). All analytes used in this screening protocol were purchased from Sigma-Aldrich and dissolved in PBS (10 mM, pH 7.4).

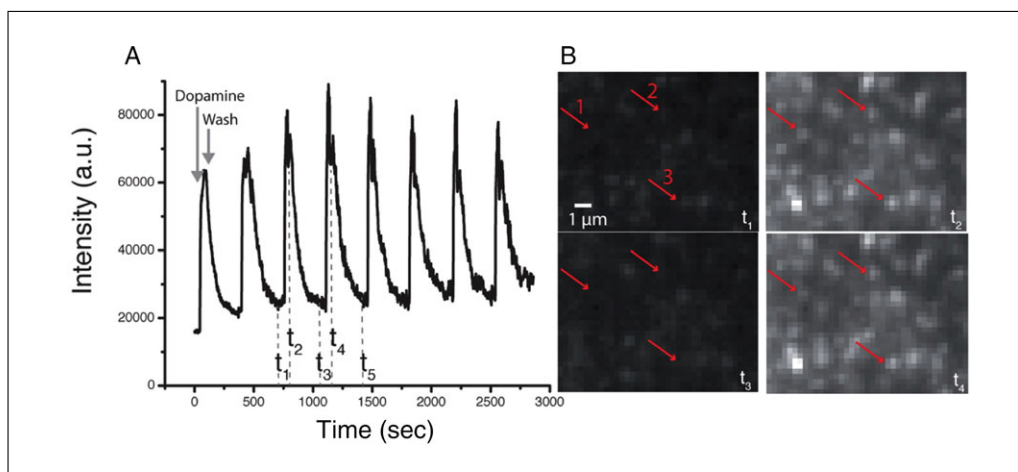


Figure 7 Reversible dopamine response of immobilized single $(GT)_{15}$ -SWCNT sensors. **(A)** Intensity time trace of 2×2 pixel (585×585 nm) region showing a single SWCNT with the surface periodically exposed to $100 \mu\text{M}$ dopamine and washed with PBS. **(B)** nIR fluorescence images of sensors that were immobilized to a surface in a flow chamber. The red arrows indicate three different carbon nanotubes; the time trace (A) shows intensity of the first SWCNT. SWCNT, single-walled carbon nanotubes; nIR, near-infrared. From Kruss et al., 2014, used with permission from the American Chemical Society.

The candidate nanosensor library for dopamine detection is composed of many different nucleic acids, phospholipids, and amphiphilic polymers (Fig. 6A and Supporting Material Fig. 1). SWCNT suspensions include a large variety of corona phases, as we had no previous information about which type of polymer would work best to recognize molecules that are structurally and functionally homologous to each other.

Screening results show that only nucleic acid-wrapped SWCNTs (N1 to N13) provide substantial fluorescence modulation upon dopamine addition. Phospholipid (PL1 to PL12) and amphiphilic polymer (P1 to P5)-wrapped SWCNTs did not produce a significant response to analytes (Fig. 6A). Among the nucleic acid-wrapped SWCNTs, $(GT)_{15}$ -wrapped SWCNT (N1) showed the highest fluorescence response to dopamine, with good selectivity and moderate interference from epinephrine. Figure 6B shows the nIR fluorescence spectrum of $(GT)_{15}$ -SWCNT before and after addition of $100 \mu\text{M}$ dopamine, and Figure 6C shows the deconvolution of each SWCNT chirality, which is used to determine the dopamine-induced fluorescence modulation of each SWCNT chirality. Our results suggest that $(GT)_{15}$ -SWCNT can be successfully used to detect nanomolar concentrations of dopamine in solution, and sub-picomolar dopamine concentrations at the single-sensor scale.

Materials

Polymer-wrapped SWCNTs (see Support Protocols 3 and 4)
 10 mM PBS, pH 7.4
 Neurotransmitters (Sigma-Aldrich; see Figure 6A)

96-well plate (Microtest 96 tissue culture plate, BD)
 Micropipet
 1D OMA V near infrared InGaAs spectrometer

Screen nanosensor library for dopamine detection

1. Dilute polymer-wrapped SWCNTs with 10 mM PBS to an SWCNT concentration corresponding to an absorbance of 0.036 at 632 nm (1 mg/liter).

Synthesis of polymer-wrapped SWCNTs is provided in Support Protocols 3 and 4.

2. Aliquot 198 μl solution from step 1 to each well of a 96-well plate.
3. Dissolve neurotransmitters in PBS and aliquot 2 μl of this solution into the wells such that the final neurotransmitter concentration is 100 μM .

Make sure to stir the wells with micropipet tip while adding the neurotransmitters to each polymer-SWCNT conjugate.

4. Measure fluorescence responses of the nine different neurotransmitters for each polymer-SWCNT combination in triplicate before and after addition of neurotransmitters with an inverted microscope coupled to a spectrometer and an InGaAs OMA V array detector (see Fig. 4A and Supporting Material Fig. 2).

Prepare fresh dopamine solutions and use within 10 min before the polymerization begins. Subsequent fluorescence measurements should take ~ 10 min.

Perform all of the experiments in PBS. Add neurotransmitters in small volumes (1 volume %), so that the change in the SWCNT concentration will be slight ($\sim 1\%$).

Make sure to wear appropriately rated eye protection when working with lasers.

Analyze fluorescence data

5. Deconvolute SWCNT emission peaks for each SWCNT chirality using custom MATLAB script (see Commentary for coding guidance).
6. To calculate fluorescence changes before and after neurotransmitter addition, compare SWCNT intensities at the fluorescence emission peak of (9,4) chirality of SWCNTs.

The (9,4) chirality peak, at ~ 1132 nm, provides the largest dopamine-induced fluorescence modulation. However, it is advised to analyze all SWCNT emission peaks to identify the peak with the largest net response to the analyte.

7. Define sensor response as $(I-I_0)/I_0$, which is the normalized difference between the final fluorescence intensity (I) and the starting intensity (I_0).
8. *Optional:* Color-code fluorescence changes as red for $\Delta I/I_0 > 0$ and blue for $\Delta I/I_0 < 0$ (see Fig. 6A). Color it so that the intensity of the color corresponds to the absolute intensity of the SWCNT-polymer response to the analyte to best visualize the results of the screen.
9. Prepare a calibration curve for dopamine response by adding varying amounts of dopamine to the polymer-wrapped SWCNT solutions. Use the same InGaAs OMA V array to detect the concentration-dependent response of the nanosensor to dopamine (see Supporting Material Fig. 4).

The same approach can be applied for other neurotransmitters, if desired.

ENCAPSULATION OF SWCNTS IN (GT)₁₅ DNA

Our screening results show that (GT)₁₅-SWCNT is a successful nanosensor to detect dopamine with high selectivity and sensitivity. This sensor can be utilized to recognize nanomolar concentrations of dopamine in solution, and sub-picomolar concentrations of dopamine at the single-sensor scale. Below, we describe the preparation of (GT)₁₅-wrapped SWCNTs through tip sonication and subsequent centrifugation. This protocol can be generalized for encapsulation with any DNA oligonucleotide and RNA.

Materials

(GT)₁₅ DNA (Integrated DNA Technologies)
0.1 M NaCl
HiPco SWCNTs (Unidym)

SUPPORT PROTOCOL 3

**Nanoparticle
Detection of
Biological
Analytes**

Sonicator (Cole-Parmer)
Beckman Coulter Ultracentrifuge
UV-vis-nIR absorption spectrometer (Shimadzu UV-3101PC)

Prepare (GT)₁₅-SWCNT

1. Dissolve (GT)₁₅ DNA at a concentration of 100 mg/ml in 0.1 M NaCl.
2. Aliquot 20 μ l DNA solution into 980 μ l 0.1 M NaCl and 1 mg HiPco SWCNTs.
Always wear gloves, lab coat, and eye protection when handling nanotubes and nanotube solutions.
Before using HiPco SWCNTs, extract non-SWCNT material by phase separation in water/hexane solution as suggested by the manufacturer (Unidym).
3. Tip-sonicate resulting suspension 10 min with 3 mm tip diameter at 40% amplitude (~5 W) in an ice bath in a fume hood.
After sonication, the sonicator's probe tip will be hot to touch.
4. Centrifuge samples two times for 90 min at 16,100 \times g at room temperature and collect supernatant.
Check each rotor bucket to ensure it is empty and free of liquid. Even a small particle or droplet in the rotor bucket could lead to off-balance of the rotor during centrifugation and severe damage to the centrifuge and/or rotor unit.
Aim to keep the top 80% to 90% of the supernatant to avoid disrupting the pellet.
As soon as centrifugation ends, the pellet will begin to dissolve into the solution. Therefore, quick separation of supernatant is required to obtain solution of ONLY single nanotubes, rather than tube bundles.
5. Analyze samples with UV-vis-nIR spectroscopy.
A sample UV-vis-nIR absorption spectrum for (GT)₁₅-SWCNT is provided as Supporting Material Figure 6. Wavelength range of 400 to 1300 nm can be used to detect the DNA peaks and characteristic multi-chirality peaks of SWCNTs.

ENCAPSULATE SWCNT IN POLYMERS

The candidate nanosensor library for dopamine detection includes suspensions with phospholipids and amphiphilic polymers, in addition to nucleic acid-wrapped SWCNTs. Even though only nucleic acid-wrapped SWCNTs provide successful dopamine detection, phospholipid and amphiphilic polymer-wrapped SWCNTs may possess detection abilities for other analytes. Below, we detail the steps needed to prepare polymer-wrapped SWCNTs that are not nucleic acid derivatives through tip sonication, centrifugation, and subsequent dialysis.

Additional Materials (also see Basic Protocol 3)

Sodium cholate (SoCh)
HiPco SWCNTs (Unidym)
Polymer of interest to conjugate to SWCNT
 Single-stranded DNA and RNA (N1 to N13; Integrated DNA Technologies)
 Phospholipids (PL1 to PL12; Avanti Polar Lipids)
 Phenoxy functionalized dextran (P1)
 FITC-PEG-FITC (fluorescein isothiocyanate-PEG-fluorescein isothiocyanate; P2)
 RITC-PEG-RITC (rhodamine isothiocyanate-PEG-rhodamine isothiocyanate; P3)

SUPPORT PROTOCOL 4

**Nanoparticle
Detection of
Biological
Analytes**

215

Boronic acid functionalized phenoxy-PPEG8 (P4; Zhang et al., 2013)
Folate-poly (ethylene glycol)-carboxylic acid (P5; Polysciotech)

Sonicator (Cole-Parmer)
Beckmann Coulter Ultracentrifuge
UV-vis-nIR absorption spectrometer (Shimadzu UV-3101PC)
3.5 kDa molecular weight cutoff dialysis bag (Spectra/Por)

Prepare polymer-wrapped SWCNTs

1. Add 1 mg/ml HiPco nanotubes to 40 ml 2 wt % SoCh in Milli-Q H₂O.

Only handle dry SWCNTs in a ventilated hood.

Always wear gloves, lab coat, and eye protection when handling nanotubes and nanotube solutions.

Before using HiPco SWCNTs, extract non-SWCNT material by phase separation in water/hexane solution as suggested by the manufacturer. SWCNT purification steps are provided in the Supporting Material.

2. Tip-sonicate solution in an ice bath with a 6-mm probe tip at 40% amplitude (~12 W) for 1 hr.
3. Centrifuge samples at 150,000 × g, 4 hr.
4. Dissolve 1 wt % polymer in a solution of SoCh-wrapped SWCNTs and dialyze against water in a 3.5 kDa molecular weight cutoff dialysis bag 5 days.
5. Analyze samples with UV-vis-nIR spectroscopy.

Wavelength range of 400 to 1300 nm can be used to detect the polymer peaks and characteristic multi-chirality peaks of SWCNTs.

SUPPORT PROTOCOL 5

USING nIRF TIRF TO INTERROGATE THE (GT)₁₅ DNA DOPAMINE-SENSING CORONA

Here we describe visualization of dopamine molecular recognition with (GT)₁₅-wrapped SWCNTs using the nIRF TIRF microscope. Our protocol is similar to probing the RITC-PEG-RITC SWCNT sensor mechanism for estradiol detection. However, in this case, the (GT)₁₅ polymer is not inherently fluorescent as in the case of RITC-PEG-RITC. Hence, we fluorescently tag our (GT)₁₅ DNA polymer via Cy3 fluorophore attachment onto the 5' end to visualize the polymer terminus conformational change at the single-molecule level.

The specificity of this (GT)₁₅ DNA-SWCNT sensor to its dopamine analyte arises from the unique conformational changes that occur in the (GT)₁₅ DNA corona phase in the presence of the analyte. We visualize (GT)₁₅ DNA conformational changes with the nIRF TIRF microscope monitoring the fluorescence of the Cy3 dye before and after dopamine addition to Cy3-(GT)₁₅ DNA-SWCNT. Before dopamine addition, immobilized (GT)₁₅-Cy3-SWCNT shows a highly quenched Cy3 signal, as expected from organic fluorophores adsorbed on the SWCNT surface. Upon addition of 100 μM dopamine, the Cy3 fluorophore is dequenched within the 100 msec acquisition frame rate, suggesting that the dopamine interacts with the terminal end of the (GT)₁₅-Cy3-SWCNT, and dequenching of Cy3 occurs as a result of fluorophore desorption from the surface of SWCNT (Fig. 8). Supporting Material Figure 7 provides further evidence that there is no large-scale displacement of the polymer from the nanotube surface. A positive control for simultaneous dequenching and desorption is conducted with 100 μM unlabeled (AC)₆ oligonucleotide that is known to be complementary to the ends of (GT)₁₅-Cy3-SWCNT. When the (AC)₆

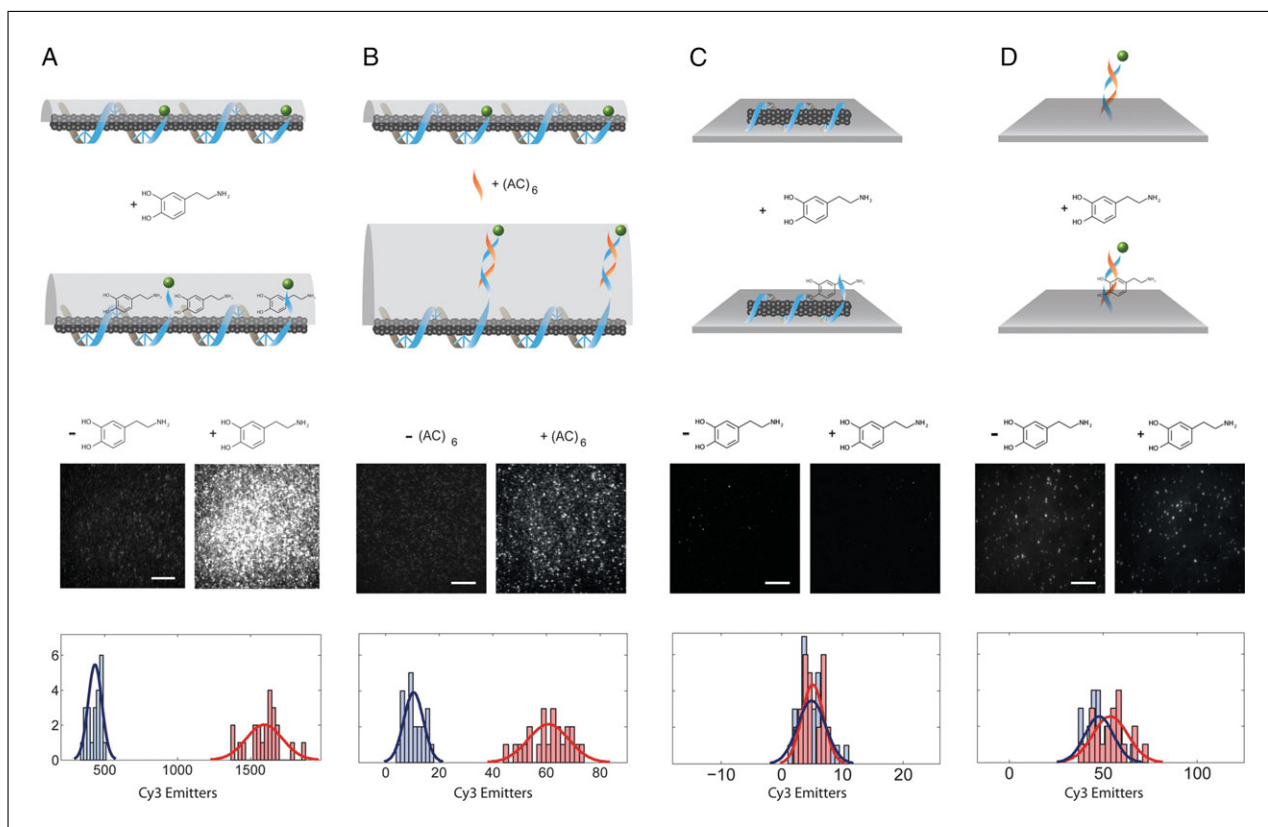


Figure 8 Dopamine-induced conformational shift of DNA. **(A)** Addition of 100 μM dopamine. **(B)** A positive control with short unlabeled complementary oligonucleotide $(\text{AC})_6$ (50 nm). **(C)** A negative control with unlabeled DNA. **(D)** A negative control with Cy3-labeled DNA on a surface without the SWCNT. The histograms show the fluorophore counts before (blue) and after (red) addition of dopamine/ $(\text{AC})_6$. From Kruss et al., 2014, used with permission from the American Chemical Society.

oligonucleotide is introduced to the same surface-immobilized $(\text{GT})_{15}$ SWCNT, dequenching of the terminal Cy3 dye from the surface is observed, suggesting that the destacking causes dequenching of the dye. Negative controls demonstrate the lack of Cy3 signal in the absence of the SWCNT or Cy3 fluorophore (Fig. 8). Below, we detail the protocol to visualize the $(\text{GT})_{15}$ -Cy3-SWCNT corona upon addition of the analyte dopamine.

Additional Materials (also see Support Protocol 2)

$(\text{GT})_{15}$ -Cy3-single-SWCNT (synthesis described in Support Protocol 3 from either Cy3-labeled $(\text{GT})_{15}$ DNA [Integrated DNA Technologies] or $(\text{GT})_{15}$ DNA [Integrated DNA Technologies] which was then labeled with Cy3 fluorophore)

531-nm narrow-bandpass filter (e.g., Semrock, cat. no. FF01-531/40-25)
 562-nm dichroic mirror (e.g., Semrock, cat. no. FF562-Di03-25 \times 36)
 593-nm bandpass filter (e.g., Semrock, cat. no. FF01-593/40-25)
 Pair of doublet lenses

Microscopy setup to visualize $(\text{GT})_{15}$ -Cy3 conformation on SWCNT upon addition of dopamine analyte

1. Surface-immobilize $(\text{GT})_{15}$ -Cy3-SWCNT as outlined in Support Protocol 2.
2. Insert a 531-nm narrow-bandpass filter before the microscope objective to tune the excitation wavelength relayed to the sample through the objective.
3. Insert a 562-nm dichroic mirror to reflect excitation wavelength while passing the Cy3 characteristic emission by allowing the transmission of wavelengths >562 nm.

4. At the emission port, insert a 593-nm bandpass filter to reflect the excitation laser light (532 nm) while passing the fluorescence emission wavelength of the Cy3 dye, which is at 570 nm.
5. Use a pair of doublet lenses to expand the $75 \times 75 \mu\text{m}$ image to fill the CDD sensor that has dimensions of $8.2 \times 8.2 \text{ mm}$ (iXon3 EMCCD, Andor Technology).
6. To image surface-immobilized (GT)₁₅-Cy3-SWCNT, change the angle of beam incidence (θ) by moving the TIR lens in the plane perpendicular to beam propagation to reach the critical angle (θ_c), at which all of the incident light is reflected from the surface and generates a field that excites fluorophores in the vicinity of glass-water interface.

This excitation method significantly lowers the fluorescent background and allows for high-resolution visualization of dynamic single-molecule behavior.

TEST REVERSIBILITY OF SWCNT-BASED MOLECULAR SENSORS

This is an optional protocol for testing the reversibility of the nanosensor if desired by the researcher. Reversibility may be desired in some sensing applications such as in dopamine detection in the brain. Dopamine is released in consecutive millisecond-scale exocytotic events in neuronal cell synapses. Hence, it is essential for a dopamine sensor to return to baseline fluorescence after responding to transient dopamine increases (Fig. 7). In Basic Protocol 4, we describe the procedure to test the reversibility of (GT)₁₅-Cy3-SWCNT sensor but this protocol can be generalized to all SWCNT-based molecular sensors.

Materials

(GT)₁₅-Cy3-SWCNT (synthesis described in Support Protocol 3 from either Cy3-labeled (GT)₁₅ DNA [Integrated DNA Technologies] or (GT)₁₅ DNA [Integrated DNA Technologies] which was then labeled with Cy3 fluorophore)
Pierce BSA-biotin (Thermo Fisher Scientific)
NeutrAvidin (Thermo Fisher Scientific)

Microfluidic chamber (Ibidi, sticky-Slide VI 0.4)
1.0 or 1.5 coverslip
Micropipet
Syringe
Harvard Apparatus PHD 2000 syringe pump

1. After preparing the microfluidic chamber as described in Support Protocol 2, flow a solution of (GT)₁₅-Cy3-SWCNT in PBS buffer through the channels and incubate 10 min to allow SWCNTs to adsorb onto the surface.
2. Place microfluidic slide with surface-immobilized SWCNT sensors on the nIRF TIRF microscope and monitor nIR emission (i.e., the sensor response). Couple a Harvard Apparatus PHD 2000 syringe pump into the inlet of the microfluidic channel with a valve to alternate between PBS buffer and 100 μM dopamine. Begin acquiring a movie of the surface-immobilized SWCNT.
3. Flow in a solution of dopamine and monitor the response of the SWCNT and the Cy3-labeled (GT)₁₅.
4. Flow in a solution of PBS to remove dopamine.
5. Repeat steps 3 and 4 as many times as desired to test the sensor.

For a good estimate of sensor response hysteresis, at least 10 iterations of steps 3 and 4 are suggested.

COMMENTARY

Background Information

Alternative methods for visualizing SWCNT corona structures

Various laboratory techniques can be employed for nanobiosensor synthesis and characterization. Alternative methods to characterize the organic corona phase around nanoparticles include mass spectrometry, atomic force microscopy (AFM), NMR, circular dichroism, absorption spectroscopy, functional group assays, cryo-transmission electron microscopy (cryo-TEM), and small-angle neutron scattering (SANS; Landry et al., 2014). These methods are generally not individually sufficient to fully characterize the corona phase surrounding the nanoparticles but will provide complementary information.

Several factors should be considered when choosing a characterization method. If single nanoparticle resolution is not required, absorption spectroscopy measurements done in bulk can provide data about the dielectric properties of the corona phase and associated solvatochromic shifts (Choi and Strano, 2007). However, if single-nanoparticle resolution is necessary, AFM could be utilized in solid phase to obtain information about the height profile of a nanotube and its solid-state corona phase (Zheng et al., 2003). The type of information needed about the nanosensor under investigation dictates the choice of the characterization technique. While mass spectrometry, gel permeation chromatography, and NMR provide data about the composition and chemical structure (Marega et al., 2010; Shannahan et al., 2013), AFM provides information about mechanical and topological features of the corona phase.

Another technique to characterize nanotubes is cryogenic transmission electron microscopy (cryo-TEM). This method can provide information on whether the nanotubes are individually suspended or they are aggregated in the solution (Moore et al., 2003; Miyauchi et al., 2004). This is a highly promising technique, as it does not require air-drying, and instead works with an instantaneous freezing of the liquid sample. Therefore, it provides information about the innate hydrated state of the nanotube and the corona phase. Like cryo-TEM, SANS also has the ability to make a distinction between different shapes and morphologies of the nanotubes (Granite et al., 2012). However, it is worthy to note that techniques such as cryo-TEM, transmis-

sion electron microscopy (TEM), AFM, and SANS only provide static information about the SWCNT corona phase and are sub-optimal to determine dynamic (time) information upon addition of analytes to SWCNT sensors.

Mitigating the cost of 2D InGaAs cameras

Alternatives exist to mitigate the high cost of 2D InGaAs cameras. The following cameras can be successfully employed to carry out the protocols we described above:

1. Zephyr 1.7-640 with a spectral range of 0.9 to 1.7 μm , pixel size of $15 \times 15 \mu\text{m}$, a 15-bit dynamic range, a 120 Hz FPS frame rate, and 250 e/p/s dark current,
2. Cougar-640 LN with a spectral range of 0.9 to 1.55 μm , pixel size of $20 \times 20 \mu\text{m}$, a 16-bit dynamic range, a 1.42 Hz FPS frame rate, and 10 e/p/s dark current,
3. NIRvana:640 with a spectral range of 0.9 to 1.7 μm , pixel size of $20 \times 20 \mu\text{m}$, a 16-bit dynamic range, a 110 Hz FPS frame rate, and 300 e/p/s dark current,
4. SWIR VGA C with a spectral range of 1 to 1.7 μm , pixel size of $25 \times 25 \mu\text{m}$, a 16-bit dynamic range, a 22 FPS frame rate, and 6241 e/p/s dark current,
5. SWIR VGA T with a spectral range of 1 to 1.7 μm , pixel size of $25 \times 25 \mu\text{m}$, a 16-bit dynamic range, a 22 FPS frame rate, and 811 e/p/s dark current.

Deconvolution and spectral analysis of SWCNT sensor fluorescence

A custom MATLAB script is written to deconvolute each SWCNT peak from the full spectra. Given a text file with information on the emission spectra of SWCNT, this code deconvolutes the spectrum into separate peaks by varying three parameters: Peak center, full width at half maximum (FWHM), and peak area and optimizing them with a nonlinear least-squares solver function of MATLAB, which is called `lsqnonlin`.

Inputs required by the code are:

1. An Excel file with FWHM values and initial guesses for peak centers (see Table 3).

First and second columns in the table contain n and m values for the chiralities, respectively. The third column contains FWHM values and the fourth column contains guessed values of peak centers.

Initial guesses are based on the calibration of the nIR spectrometer based on a known light source (i.e., Xenon lamp) and identification of

Table 3 Full Width-Half Maximum (FWHM) Values and Initial Guesses for Peak Centers for MATLAB Code of Deconvolution^a

<i>n</i>	<i>m</i>	FWHM	Peak center (nm)
8	3	19.18	972
6	5	24.46	991
7	5	25.17	1040
10	2	23.44	1076
9	4	18.66	1130
7	6	23.49	1136
12	1	23.66	1204
11	3	21.49	1230
10	5	20.49	1258.448
8	7	27.22	1280.579

^aThe first and second columns contain *n* and *m* values for each of the SWCNT chiralities, respectively, where *n* and *m* are integers that describe the chiral vector, (*n,m*), and are part of the vector equation, $R = na_1 + ma_2$.

SWCNT peaks from an SDS-SWCNT sample taken post-calibration with Xenon lamp.

2. A Text file with the spectrum data.

First column contains wavelengths and second column contains intensities.

Outputs produced by the code:

1. Individual deconvoluted Gaussians,
2. Wavelength versus Intensity for each chirality.

Critical Parameters

Polymerization of dopamine

Time-dependent variations in the absolute magnitude of the sensor response are observed due to dopamine polymerization in solution. This caution is extended to any analyte that can undergo changes in solution over time. In the case of dopamine, sensor response decreases with time as a result of quenching caused by the dopamine polymerization product. The sensor response over the course of 90 min is shown in Supporting Information Figure 3. The data for the first 10 min is experimental, and the rest is predicted by a kinetic model (see Kruss et al., 2014). At early time points, fluorescence increase is limited by dopamine diffusion to the sensor, and hence the response is instantaneous. Over the course of 90 min, the sensor response decreases from 80% to almost 60% due to gradual dopamine polymerization.

This demonstrates that fluorescence can depend on the freshness of the dopamine solution and the time required to carry out the experi-

ment. An increase in dopamine solution optical density has been observed throughout the course of an hour and precipitation after a day. As a result, only freshly prepared dopamine should be used for screening, as indicated in the protocol.

Saturation of sensor response

The calibration curve for sensor response can be prepared based on the kinetic adsorption model in which the analyte binds to the available recognition sites on the SWCNT sensor with an instantaneous reaction (Supporting Material Fig. 4). This model shows that even for very dilute dopamine concentrations (100 pM), there is a fluorescence increase of ~5%, which is a promising result to be able to detect small dopamine concentrations in the brain. The sensor response demonstrates a linear trend for dopamine concentrations between 10 nM and 10 μM. However, the sensor response saturates when > 10 μM dopamine is administered. Therefore, this particular sensor should not be used to measure concentrations > 10 μM based solely on fluorescence data. We emphasize the importance of knowing biologically relevant concentrations of the analyte and ensuring the sensor response is maximal in this concentration range.

Troubleshooting

Purity of SWCNTs

Chemical vapor deposition (CVD) is an important and commonly used method to grow carbon nanotubes. CVD uses a metal-based catalyst to grown carbon nanotubes from hydrocarbon feed stocks, residual amounts of which may be present in the final product. Furthermore, CVD growth of SWCNTs also produces amorphous carbon, small amounts of which may also be present in the final product. Amorphous carbon can bind analytes without any response and metal-based catalysts quench the fluorescence of carbon nanotubes. Purchased SWCNTs may also contain methanol as an organic binder. Therefore, SWCNTs have to be washed prior to use to remove these impurities. A protocol for washing carbon nanotubes can be found in the Supporting Material.

Cytotoxicity of carbon nanotubes during in vivo applications

To prevent possible cytotoxicity, surface passivation of carbon nanotubes for in vivo applications can be carried out by functionalizing the surface of the nanotubes with poly(ethylene) glycol (PEG), in a process

called PEGylation. PEGylated carbon nanotubes have been shown to have higher solubility and lower cytotoxicity than their non-PEGylated versions (Liu et al., 2009b). PEGylation may be necessary for eventual in vivo studies of the sensors described in this protocol if the side effects of non-PEGylated nanosensors are found to be severe. Here, we emphasize the need to choose a non-covalent PEGylation scheme that retains the fluorescence properties of carbon nanotubes. The non-covalent PEGylation of the (GT)₁₅-SWCNT dopamine sensor is provided in the Supporting Material.

Lack of selectivity in screening

In all of the protocols provided, the signal observed from SWCNT sensors arises from the fluorescence response of the multi-chirality SWCNT sample with multiple peaks of nIR emission. When this type of sensor is introduced into a complex biological environment that has many analogues of the analyte of interest, the sensor response may not be limited to the analyte of interest. As can be seen from Figure 6A, the sensor responds to many analytes with different intensities. To increase the selectivity in screening, a ratiometric approach can be used in which specific chiralities respond in a unique way to an analyte, providing an internal control that enables ratiometric sensing. Ratiometric sensing approaches require that SWCNTs be separated into distinct chiral species. For more information about automated and scalable chromatographic SWCNT separation protocols see Flavel et al. (2014), Jain et al. (2014), and Giraldo et al. (2015).

Anticipated Results

Basic Protocol 1 offers a novel way to visualize and characterize both the corona phase surrounding the nanotubes and the nanotubes themselves with high spatial and temporal resolution. Basic Protocols 2 and 3 generate synthetic heteropolymer wrapped SWCNTs that are able to recognize specific molecules such as estradiol and dopamine. Basic Protocol 4 describes the procedure to test the reversibility of SWCNT-based molecular sensors. Molecular recognition of other important bio-analytes can also be achieved by synthesizing new polymer-SWCNT screening libraries as described in this protocol. These methods can find use in low-cost medical diagnostic applications and spatiotemporal neurotransmitter detection near synapses or in neural networks.

Time Considerations

In the presented protocols, sonication usually requires 3 hr, dialysis takes 3 to 5 days, and the microscopy procedures require 2 hr. Once all necessary reagents are obtained, the individual protocols can be completed within a week. However, readers should keep in mind that building the microscopes described herein can take several months.

Supporting Materials

All supporting material figure and text files discussed in this article can only be accessed from the online version of this article.

Acknowledgment

This work was supported by a Burroughs Wellcome Fund Career Award at the Scientific Interface (CASI), a Brain and Behavior Research foundation young investigator grant, and a Beckman Foundation Investigator Award. A.G.B. acknowledges a U.C. Berkeley Chancellor's Fellowship and an NSF Graduate Research Fellowship. G.S.D. acknowledges a Schlumberger Foundation Fellowship. A.G.B. wrote the introduction, Basic Protocols 1 and 2, and Support Protocols 1 and 2. G.S.D. wrote Basic Protocols 3 and 4, Support Protocols 3, 4, and 5, and commentary parts of this paper. A.G.B. and G.S.D. collaboratively edited the manuscript with guidance from M.P.L. The authors would like to thank Roger Chang for helpful discussions.

Conflicts of Interest Statement

Authors of this manuscript declare no conflicts of interest.

Literature Cited

- Adams, K.L., Puchades, M., and Ewing, A.G. 2008. In vitro electrochemistry of biological systems. *Annu. Rev. Anal. Chem. (Palo Alto, Calif.)* 1:329-355. doi: 10.1146/annurev.anchem.1.031207.113038.
- Bachilo, S.M., Strano, M.S., Kittrell, C., Hauge, R.H., Smalley, R.E., and Weisman, R.B. 2002. Structure-assigned optical spectra of single-walled carbon nanotubes. *Science* 298:2361-2366. doi: 10.1126/science.1078727.
- Bisker, G., Ahn, J., Kruss, S., Ulissi, Z.W., Salem, D.P., and Strano, M.S. 2015. A mathematical formulation and solution of the CoPh-MoRe inverse problem for helically wrapping polymer corona phases on cylindrical substrates. *J. Phys. Chem. C* 119:13876-13886. doi: 10.1021/acs.jpcc.5b01705.
- Bisker, G., Dong, J., Park, H.D., Iverson, N.M., Ahn, J., Nelson, J.T., Landry, M.P., Kruss, S., and Strano, M.S. 2016. Protein-targeted corona phase molecular recognition. *Nat. Commun.* 7. doi:10.1038/ncomms10241.

- Cho, E.J., Lee, J.-W., and Ellington, A.D. 2009. Applications of aptamers as sensors. *Annu. Rev. Anal. Chem.* 2:241-264. doi: 10.1146/annurev.anchem.1.031207.112851.
- Choi, J.H. and Strano, M.S. 2007. Solvatochromism in single-walled carbon nanotubes. *Appl. Phys. Lett.* 90:223114. doi: 10.1063/1.2745228.
- Flavel, B.S., Moore, K.E., Pfohl, M., Kappes, M.M., and Hennrich, F. 2014. Separation of Single-walled carbon nanotubes with a gel permeation chromatography system. *ACS Nano* 8:1817-1826. doi: 10.1021/nn4062116.
- Giraldo, J.P., Landry, M.P., Kwak, S.Y., Jain, R.M., Wong, M.H., Iverson, N.M., Ben-Naim, M., and Strano, M.S. 2015. A ratiometric sensor using single chirality near-infrared fluorescent carbon nanotubes: Application to in vivo monitoring. *Small* 11:3973-3984. doi: 10.1002/sml.201403276.
- Granite, M., Radulescu, A., and Cohen, Y. 2012. Small-angle neutron scattering from aqueous dispersions of single-walled carbon nanotubes with Pluronic F127 and poly(vinylpyrrolidone). *Langmuir* 28:11025-11031. doi: 10.1021/la302307m.
- Hong, G., Diao, S., Antaris, A.L., and Dai, H. 2015. Carbon nanomaterials for biological imaging and nanomedicinal therapy. *Chem. Rev.* 115:10816-10906. doi: 10.1021/acs.chemrev.5b00008.
- Jain, R.M., Tvrđy, K., Han, R., Ulissi, Z., and Strano, M.S. 2014. Quantitative theory of adsorptive separation for the electronic sorting of single-walled carbon nanotubes. *ACS Nano* 8:3367-3379. doi: 10.1021/nn4058402.
- Joo, C. and Ha, T. 2012. Single-molecule FRET with total internal reflection microscopy. *Cold. Spring. Harb. Protoc.* 2012. doi: 10.1101/pdb.top072058.
- Kim, D., Koseoglu, S., Manning, B.M., Meyer, A.F., and Haynes, C.L. 2011. Electroanalytical eavesdropping on single cell communication. *Anal. Chem.* 83:7242-7249. doi: 10.1021/ac200666c.
- Kruss, S., Landry, M.P., Vander Ende, E., Lima, B.M.A., Reuel, N.F., Zhang, J., Nelson, J., Mu, B., Hilmer, A., and Strano, M. 2014. Neurotransmitter detection using corona phase molecular recognition on fluorescent single-walled carbon nanotube sensors. *J. Am. Chem. Soc.* 136:713-724. doi: 10.1021/ja410433b.
- Landry, M.P., Kruss, S., Nelson, J.T., Bisker, G., Iverson, N.M., Reuel, N.F., and Strano, M.S. 2014. Experimental tools to study molecular recognition within the nanoparticle corona. *Sensors* 14:16196-16211. doi: 10.3390/s140916196.
- Liu, Y., Dong, X., and Chen, P. 2012. Biological and chemical sensors based on graphene materials. *Chem. Soc. Rev.* 41:2283-2307. doi: 10.1039/C1CS15270J.
- Liu, Z., Tabakman, S., Welscher, K., and Dai, H. 2009a. Carbon nanotubes in biology and medicine: In vitro and in vivo detection, imaging and drug delivery. *Nano. Res.* 2:85-120. doi: 10.1007/s12274-009-9009-8.
- Liu, Z., Tabakman, S.M., Chen, Z., and Dai, H. 2009b. Preparation of carbon nanotube bioconjugates for biomedical applications. *Nat. Protoc.* 4:1372-1381. doi: 10.1038/nprot.2009.146.
- Marega, R., Aroulmoji, V., Bergamin, M., Feruglio, L., Dinon, F., Bianco, A., Murano, E., and Prato, M. 2010. Two-dimensional diffusion-ordered NMR spectroscopy as a tool for monitoring functionalized carbon nanotube purification and composition. *ACS Nano* 4:2051-2058. doi: 10.1021/nn100257h.
- Miyauchi, Y., Chiashi, S., Murakami, Y., Hayashida, Y., and Maruyama, S. 2004. Fluorescence spectroscopy of single-walled carbon nanotubes synthesized from alcohol. *Chem. Phys. Lett.* 387:198-203. doi: 10.1016/j.cplett.2004.01.116.
- Moore, V.C., Strano, M.S., Haroz, E.H., Hauge, R.H., Smalley, R.E., Schmidt, J., and Talmon, Y. 2003. Individually suspended single-walled carbon nanotubes in various surfactants. *Nano Lett.* 3:1379-1382. doi: 10.1021/nl034524j.
- Oliveira, S.F., Bisker, G., Bakh, N.A., Gibbs, S.L., Landry, M.P., and Strano, M.S. 2015. Protein functionalized carbon nanomaterials for biomedical applications. *Carbon* 95:767-779. doi: 10.1016/j.carbon.2015.08.076.
- Peluso, P., Wilson, D.S., Do, D., Tran, H., Venkatasubbaiah, M., Quincy, D., Heidecker, B., Poindexter, K., Tolani, N., and Phelan, M. 2003. Optimizing antibody immobilization strategies for the construction of protein microarrays. *Anal. Biochem.* 312:113-124. doi: 10.1016/S0003-2697(02)00442-6.
- Perry, M., Li, Q., and Kennedy, R.T. 2009. Review of recent advances in analytical techniques for the determination of neurotransmitters. *Anal. Chim. Acta* 653:1-22. doi: 10.1016/j.aca.2009.08.038.
- Rodriguez, P.C., Pereira, D.B., Borgkvist, A., Wong, M.Y., Barnard, C., Sonders, M.S., Zhang, H., Sames, D., and Sulzer, D. 2013. Fluorescent dopamine tracer resolves individual dopaminergic synapses and their activity in the brain. *Proc. Natl. Acad. Sci. U.S.A.* 110:870-875. doi: 10.1073/pnas.1213569110.
- Roy, R., Hohng, S., and Ha, T. 2008. A practical guide to single-molecule FRET. *Nat. Methods* 5:507-516. doi: 10.1038/nmeth.1208.
- Saerens, D., Huang, L., Bonroy, K., and Muyldermans, S. 2008. Antibody fragments as probe in biosensor development. *Sensors* 8:4669-4686. doi: 10.3390/s8084669.
- Salem, D.P., Landry, M.P., Bisker, G., Ahn, J., Kruss, S., and Strano, M.S. 2016. Chirality dependent corona phase molecular recognition of DNA-wrapped carbon nanotubes. *Carbon* 97:147-153. doi: 10.1016/j.carbon.2015.08.075.

- Shannahan, J.H., Brown, J.M., Chen, R., Ke, P.C., Lai, X., Mitra, S., and Witzmann, F.A. 2013. Comparison of nanotube-protein corona composition in cell culture media. *Small* 9:2171-2181. doi: 10.1002/smll.201202243.
- Skottrup, P.D., Nicolaisen, M., and Justesen, A.F. 2008. Towards on-site pathogen detection using antibody-based sensors. *Biosens. Bioelectron.* 24:339-348. doi: 10.1016/j.bios.2008.06.045.
- Snow, E.S., Perkins, F.K., Houser, E.J., Badescu, S.C., and Reinecke, T.L. 2005. Chemical detection with a single-walled carbon nanotube capacitor. *Science* 307:1942-1945. doi: 10.1126/science.1109128.
- Telford, W.G., Subach, F.V., and Verkhusha, V.V. 2009. Supercontinuum white light lasers for flow cytometry. *Cytometry Part A* 75:450-459. doi: 10.1002/cyto.a.20687.
- Zhang, J., Landry, M.P., Barone, P.W., Kim, J.-H., Lin, S., Ulissi, Z.W., Lin, D., Mu, B., Boghosian, A.A., and Hilmer, A.J. 2013. Molecular recognition using corona phase complexes made of synthetic polymers adsorbed on carbon nanotubes. *Nat. Nanotechnol.* 8:959-968. doi: 10.1038/nnano.2013.236.
- Zheng, M., Jagota, A., Strano, M.S., Santos, A.P., Barone, P., Chou, S.G., Diner, B.A., Dresselhaus, M.S., Mclean, R.S., and Onoa, G.B. 2003. Structure-based carbon nanotube sorting by sequence-dependent DNA assembly. *Science* 302:1545-1548. doi: 10.1126/science.1091911.